University of South Bohemia, Ceske Budejovice

Institute of Physical Biology, Nove Hrady

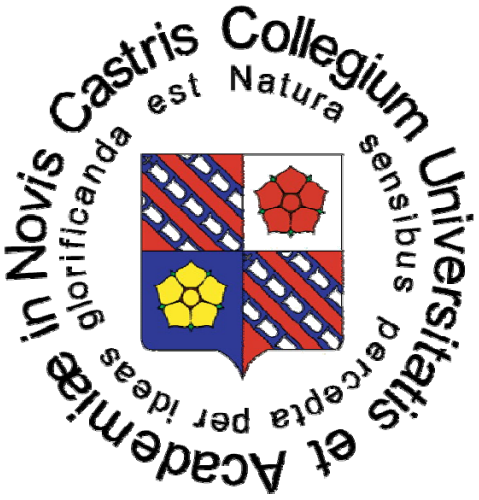

Ph.D. thesis

Selected mutants of haloalkane dehalogenase (DhaA) as a subject for structural and functional studies

Alena Stsiapanava

Supervisor: **Assoc. Prof. Ivana Kuta Smatanova, Ph.D.**

Institute of Physical Biology, University of South Bohemia Ceske Budejovice, Zamek 136, 373 33 Nove Hrady, Czech Republic
Institute of Systems Biology and Ecology, v.v.i., Academy of Science of the Czech Republic, Zamek 136, 373 33 Nove Hrady, Czech Republic

Nove Hrady, 2010

PROHLÁŠENÍ

Prohlašuji, že svoji disertační práci jsem vypracovala samostatně pouze s použitím pramenů a literatury uvedených v seznamu citované literatury.

Prohlašuji, že v souladu s § 47b zákona č. 111/1998 Sb. v platném znění souhlasím se zveřejněním své disertační práce "Selected mutants of haloalkane dehalogenase (DhaA) as a subject for structural and functional studies" v úpravě vzniklé vypuštěním Paper I, Paper II, Paper III, Paper IV a Paper V, archivovaných Ústavem fyzikální biologie JU, elektronickou cestou ve veřejně přístupné části databáze STAG provozované Jihočeskou univerzitou v Českých Budějovicích na jejích internetových stránkách, a to se zachováním mého autorského práva k odevzdanému textu této kvalifikační práce. Souhlasím dále s tím, aby toutéž elektronickou cestou byly v souladu s uvedeným ustanovením zákona č. 111/1998 Sb. zveřejněny posudky školitele a oponentů práce i záznam o průběhu a výsledku obhajoby kvalifikační práce. Rovněž souhlasím s porovnáním textu mé kvalifikační práce s databází kvalifikačních prací Theses.cz provozovanou Národním registrem vysokoškolských kvalifikačních prací a systémem na odhalování plagiátů.

V Nových Hradech, 24. listopadu 2010 . . . . . .

Podpis studenta

Aknowledgements

I would like to thank everyone who has contributed to my research work that has been done at the **Dept. Structure and Function of Proteins** in the **Institute of Physical Biology.**

I am thankful to **Ivana Kuta Smatanova** for accepting me as PhD student, providing convenient environment for my work in the field of macromolecular crystallization and support during my study in Nove Hrady.

I acknowledge **Ivana Tomcova** for her practical advises during my initial crystallization experiments.

I am grateful to my colleague from Prague **Jan Dohnalek** for teaching and helping me with determination of atomic resolution structures of DhaA proteins on all steps, from the data processing till the analysis of results. I would like to express my gratitude for his appropriate advices and suggestions that have helped me in solving of various crystallographic problems and for all crystallographic knowledge I have got during our work and communication. Also I want to thank for Jan's patience when he has answered on my numerous crystallographic questions.

I would also like to thank my colleague from Granada - **Jose Gavira** for helping me with refinement and analysis of the structures of two proteins of interest.

I give gratitude to **Jeroen R. Mesters** for introducing me to *SHELXL* program and our scientific discussions during my two weeks practice in Institute of Biochemistry, University of Luebeck, Germany.

I also wish to acknowledge the contributions, advices and suggestions of my colleagues from Brno: **Jiri Damborsky, Radka Chaloupkova** and **Tana Koudelakova.** Thanks them for introducing me to the field of molecular biology.

I want to give my thanks to **Monica Strakova** and **Eva Hrdlickova** from Brno for their help with protein expression and purification**.**

Scientific stuff of EMBL, Hamburg, and **BESSY, Berlin**, beamlines were extremely helpful in assisting of diffraction measurements.

I would like to thank also my present colleagues and friends at the department for their comprehensive suggestions, warm encouragement and support in our daily life in the castle.

Thank to **the technical** and **administrative stuff** of the Castle for their availability and kindness and the head of the Institute of Physical Biology **Dalibor Stys**.

Annotation

Structural biology is one of the most quickly growing fields of research in life sciences. X-ray diffraction analysis is the technique that allows direct visualization of protein structure at the atomic or near-atomic level. Structure solution of proteins and protein complexes by X-ray crystallography provides important insights into their mode of action. The haloalkane dehalogenase proteins represent objects of interest for protein engineering studies, attempting to improve their catalytic efficiency or broaden their substrate specificity towards environmental pollutants. In the present study, the structures of three haloalkane dehalogenase DhaA mutants DhaA04, DhaA14 and DhaA15 at atomic resolution are reported and compared to explore the effect of mutations on the enzymatic activity of modified proteins from a structural perspective. Besides that, in this work, the crystallization and initial X-ray diffraction characterization of DhaA wild type and its mutant variant DhaA13 in complex with environmental pollutant 1,2,3-trichloropropane and the crystallization of DhaA13 in complex with the fluorescence dye coumarin are described.

Anotace

Strukturní biologie je jednou z nejrychleji se rozvíjejících oblastí v biologických vědách. Rentgenová difrakční analýza je technika, která umožňuje přímou vizualizaci proteinových struktur na atomárním rozlišení. Řešení struktur proteinů a proteinových komplexů pomocí metod rentgenové difrakce poskytuje důležitý pohled na způsob jejich fungování. Haloalkan dehalogenázy jsou proteiny mající velký význam pro studie v proteinovém inženýrství, kdy je zájem soustředěn na zvýšení jejich katalytické účinnosti nebo rozšíření jejich substrátové specificity k ekologickým polutantům. V předkládané práci jsou detailně popsány nové struktury tří mutantních haloalkan dehalogenáz DhaA04, DaA14 a DhaA15, které byly vyřešeny na atomárním rozlišení. Struktury jsou vzájemně srovnány s cílem objasnit efekt mutací na enzymovou aktivitu modifikovaných proteinů. Kromě těchto struktur jsou v práci charakterizovány krystalizační a strukturní studie divokého typu DhaA a jeho mutantní formy DhaA13 se substrátem 1,2,3-trichloropropanem a krystalizační experimenty s DhaA13 v komplexu s fluorescenčním barvivem kumarinem.

List of papers

I. **Crystals of DhaA mutants from *Rhodococcus rhodochrous* NCIMB 13064 diffracted to ultrahigh resolution: crystallization and preliminary diffraction analysis.** Stsiapanava, A., Koudelakova, T., Lapkouski, M., Pavlova, M., Damborsky, J. and Kuta Smatanova, I., *Acta Crys.,* F**64**, 137-140 (2008).

II. **Pathways and Mechanisms for Product Release in the Engineered Haloalkane Dehalogenases Explored using Classical and Random Acceleration Molecular Dynamics Simulations.** Klvana, M., Pavlova, M., Koudelakova, T., Chaloupkova, R., Dvorak, P., Stsiapanava, A., Kuty, M., Kuta Smatanova, I., Dohnalek, J., Kulhanek, P., Wade, R. C. and Damborsky, J., *J. Mol. Biol.* **392**, 1339-1356 (2009).

III. **Atomic resolution studies of engineered haloalkane dehalogenases DhaA04, DhaA14 and DhaA15 carrying mutations in access tunnels.** Stsiapanava, A., Dohnalek, J., Gavira, J. A., Kuty, M., Koudelakova, T., Damborsky, J. and Kuta Smatanova, I., *Acta Cryst*. D**66,** 962-969 (2010).

IV. **Crystallization and preliminary X-ray diffraction analysis of the wild type haloalkane dehalogenases DhaA and the variant DhaA13 complexed with different ligands.** Stsiapanava, A., Chaloupkova, R., Jesenska, A., Brynda, J., Weiss, M. S., Damborsky, J. and Kuta Smatanova, I., *manuscript submitted to Acta Cryst F* (2010)

V. **Crystallization and crystallographic analyses of the *Rhodococcus rhodochrous* NCIMB 13064 mutant DhaA31 and its complex with 1, 2, 3-trichloropropane**. Lahoda, M., Chaloupkova, R., Stsiapanava, A., Damborsky, J. and Kuta Smatanova**,** I., *manuscript prepared for submission to Acta Cryst F* (2010)

My contribution to the papers

In **papers I, III** and **IV** I was involved in the experimental planning, did the significant part of the experimental work and data analysis. I wrote **papers I, III** and **IV**. In **paper V** I was involved in part of experimental work and data analysis. In **paper II** my experimental data was used.

On behalf of the co-authors, the above-mentioned declaration was confirmed by

Assoc. Prof. Ivana Kuta Smatanova, Ph.D
(supervisor and co-author of the papers)

Table of contents

1. Introduction……. 8

2. Haloalkane dehalogenases ……. 10

2.1. Structure of haloalkane dehalogenases ……. 10

2.2. Catalytic mechanism of haloalkane dehalogenases ……... 12

2.3. Applications of haloalkane dehalogenases …… 14

2.4. Haloalkane dehalogenase DhaA from *Rhodococcus rhodochrous* NCIMB 13064 …… 16

2.4.1. Structure and functions of DhaA enzyme……... 16

2.4.2. DhaA protein variants…….. 19

2.4.2.1. DhaA04, DhaA14 and DhaA15 variants……. 19

2.4.2.2. DhaA13 protein variant……... 21

3. Experimental methods……. 23

3.1. Crystallization of biological macromolecules and crystal structure determination…… 23

3.1.1. Macromolecular crystallization……... 24

3.1.1.1. Basic of method……... 24

3.1.1.2. Crystallization techniques…… 25

3.1.1.3. Finding optimal conditions for crystal growth…… 26

3.1.2. Crystal structure determination…… 27

3.1.2.1. Crystallographic data collection…….. 27

3.1.2.2. Scattering by a crystal…….. 29

3.1.2.3. The electron density equation and solving the phase problem…… 30

3.1.2.3.1. Isomorphous replacement……. 31

3.1.2.3.2. Anomalous diffraction…….. 32

3.1.2.3.3. Molecular replacement……. 33

3.1.2.4. Model building and refinement……... 33

4. Summary of papers …….. 35

References……..... 39

1. Introduction

The activity and substrate specificities of enzymes involved in the catalysis of biodegradation reactions can determine the biodegradability of organic substances in the environment. Chlorinated aliphatic xenobiotic compounds form group of chemicals, which were unknown to nature before humans started their industrial production. It is possible that microorganisms did not have a sufficient amount of time to evolve the enzymes with specificities and activities required for the catalysis of these synthetic compounds and their metabolic intermediates (Damborsky & Koca, 1999). Combining rational protein design with directed evolution provides a very efficient two-step approach for engineering proteins with desired activities (Pavlova *et al*., 2009). Modeling mutant proteins and binding of various substrates should further help to suggest specific mutations yielding activity with substrates that are not hydrolyzed by present enzymes (Pries *et al*., 1994b).

Haloalkane dehalogenases (EC 3.8.1.5) comprise a group of enzymes that hydrolyzed carbon-halogen bonds in a wide range of haloalkanes, some of which are environmental pollutants. The potential use of haloalkane dehalogenases in bioremediation applications has stimulated intensive investigation of these enzymes, and there is growing interest in the application of these enzymes as industrial biocatalysts (Bosma *et al*., 2003). The differences in substrate specificity and efficiency of haloalkane dehalogenases reactions originating from the size and geometry of an active site and its entrances and the efficiency of the transition state and halide ion stabilization by active site residues. Mechanisms of ligand exchange between buried active sites and bulk solvent and the effects of mutations on the exchange process are often less well understood than the mechanisms of chemical reactions taking place in the active sites (Klvana *et al*., 2009). Since structure is related to function in the sense that it is the basis of it, one can learn about the function of a biomacromolecule by determining and carefully interpreting its

structure. To obtain this information on an atomic level the use of X-ray crystallography is the most sufficient technique.

Haloalkane dehalogenase DhaA from *R. rhodochrous* NCIMB 13064 was described as the first dehalogenase enzyme with ability to slowly convert groundwater contaminant 1,2,3-trichloropropane (TCP) under laboratory conditions (Bosma *et al*., 1999; Bosma *et al*., 2002; Janssen, 2004). In present study, we report crystallization and preliminary X-ray diffraction characterization of wild type DhaA and its variant DhaA13, carrying mutation in the catalytic residue, complexed with different ligands, as well as crystallization and crystallographic analysis of three DhaA protein variants (DhaA04, DhaA14 and DhaA15) with modified access routes connecting the buried active site cavity with the surrounded solvent.

2. Haloalkane dehalogenases

2.1. Structure of haloalkane dehalogenases

Haloalkane dehalogenases (EC 3.8.1.5) belong to the α/β-hydrolase fold superfamily (Ollis *et al*., 1992; Nardini & Dijsktra, 1999). Structurally, the members of this superfamily consist of two domains: an α/β-hydrolase fold domain and a helical cap domain.

The α/β-hydrolase core domain is conserved among the members of superfamily and forms the hydrophobic core to provide the skeleton for hanging on the catalytic residues in a spatial arrangement suitable for catalysis. The core domain of haloalkane dehalogenases is composed of an eight-stranded β-sheet with seven parallel and one antiparallel strand surrounded by α-helices.

The catalytic residues of haloalkane dehalogenases are arranged in catalytic pentad. It is composed of three residues that influence the nucleophilic attack: nucleophile (Asp), base (His) and catalytic acid (Asp or Glu), and two halide-stabilizing residues (Trp and Trp or Asn). While the conserved nucleophile is located after the strand β5 and the conserved base is always after the strand β8, the catalytic acid is either after the strand β6 or after the strand β7. The nucleophile is always located in a very sharp turn, called the "nucleophile elbow", where it can be easily approached by the substrate, as well as by the hydrolytic water molecules. The "nucleophile elbow" is the most conserved structure within the α/β-hydrolase fold. One of the halide-binding residues is invariable and flanks the nucleophile. The second halide-stabilizing residue is variable and located in the cap domain or after the strand β3. The regions around the two halide-binding residues and the nucleophile elbow are highly conserved and create the "oxyanion hole", which is needed to stabilize the negatively charged transition state that occurs during hydrolysis.

The cap domain is composed of a few helices and is supposed to be important for substrate specificity in haloalkane dehalogenases. This domain appears to be strongly variable among the different classes of these hydrolases. The most flexible

part of the haloalkane dehalogenases is the random coil interconnecting two domains. The active site cavity is located between domains and connected with surrounding solvent by the several tunnels (Janssen, 2004; Ollis *et al*., 1992; Nardini & Dijsktra, 1999; Damborsky & Koca, 1999; Chovancova *et al*., 2007; Otyepka&Damborsky, 2002) (**Fig. 1**).

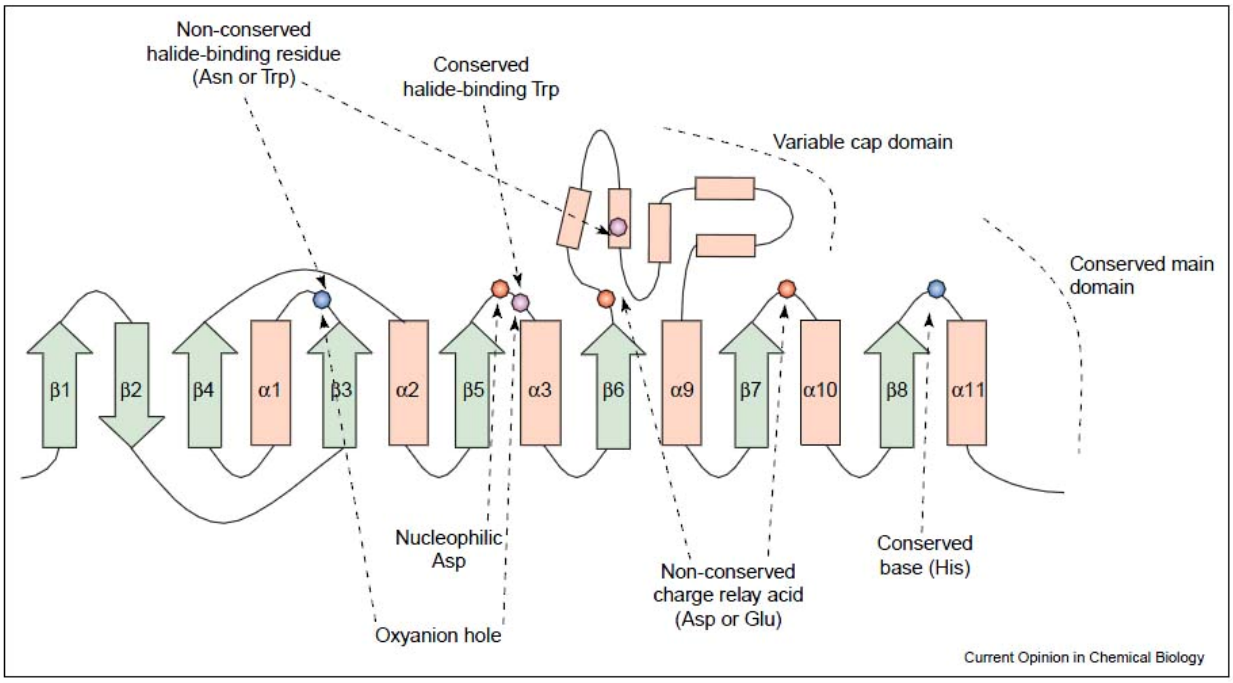

Figure 1. *The topological arrangement of secondary structure elements of haloalkane dehalogenases (adapted from Janssen, 2004).*

Based on phylogenetic analyses, Chovancova *et al*. (2007) proposed that haloalkane dehalogenases should be divided into three subfamilies marked as HLD-I, HLD-II, and HLD-III, of which HLD-I and HLD-III were predicted to be sister-groups (**Fig. 2**). Nucleophile, catalytic base, and one halide-stabilizing residue are conserved among all subfamilies, whereas the catalytic acid and second halide-stabilizing residue differ among subfamilies. The most of the biochemically characterized haloalkane dehalogenases are found in the HLD-II subfamily (Chovancova *et al*., 2007).

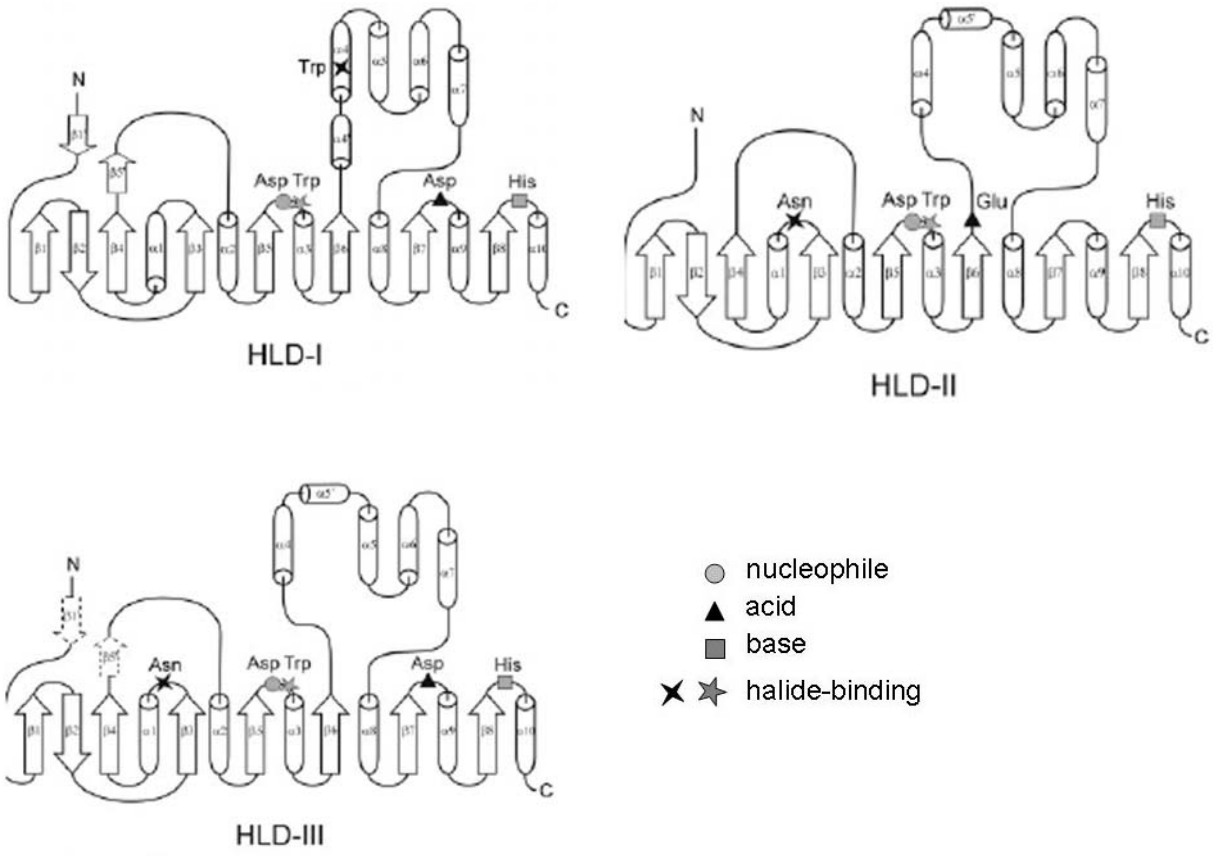

Figure 2. *The topological arrangement of secondary structure elements in individual haloalkane dehalogenase subfamilies (HLD-I, HLD-II, and HLD-III). Positions of catalytic pentad residues are indicated by symbols (adapted from Chovancova et al., 2007).*

2.2. Catalytic mechanism of haloalkane dehalogenases

Haloalkane dehalogenases convert a broad spectrum of haloalkanes to the corresponding alcohols by hydrolytic cleavage of the carbon-halogen bond (**Fig. 3**). There is no evidence indicating the involvement of cofactors or metal ions in the catalytic mechanism (Verschueren *et al.*, 1993; Janssen *et al.,* 1994). The catalytic water of haloalkane dehalogenases is significantly less mobile than other water molecules in the active site. Exchange of water molecules between the active-site cavity and bulk solvent differs among dehalogenases as the consequence of the different mobility of the cap domains and different number of entrance tunnels (Otyepka&Damborsky, 2002).

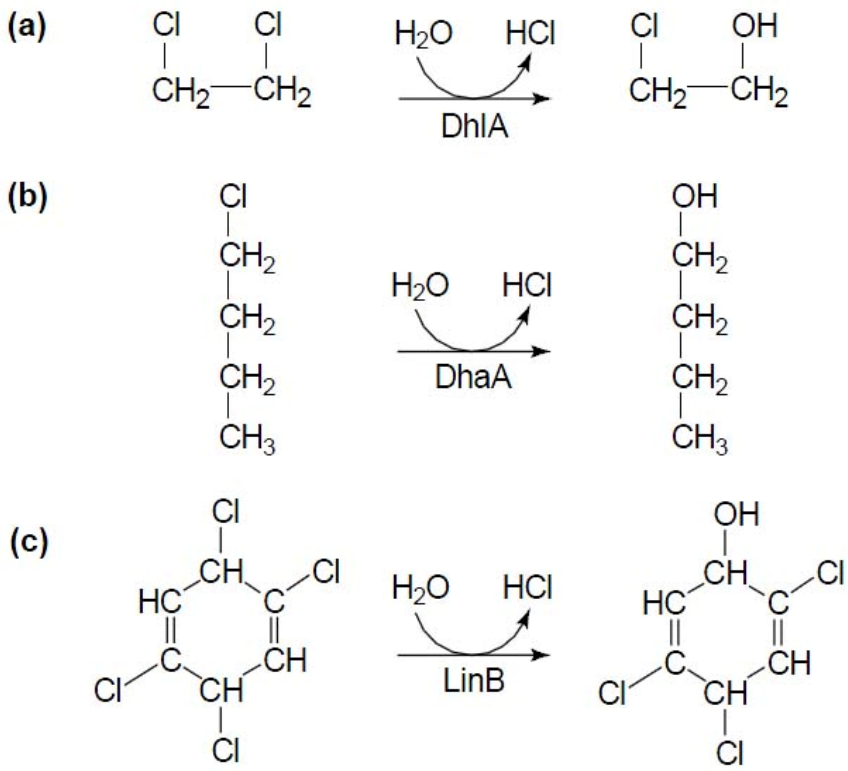

Figure 3. *Examples of dehalogenation reactions in bacterial cultures from (a) Xanthobacter autotrophicus (DhlA), (b) Rhodococcus erythropolis (DhaA), (c) Spingomonas paucimobilis (LinB) (adapted from Janssen, 2004).*

The reaction mechanism of haloalkane dehalogenases has been proposed from X-ray crystallography (Verschueren *et al.*, 1993) and site-directed mutagenesis experiments (Pries *et al.*, 1994a). Catalysis proceeds by the nucleophilic attack of the carboxylate oxygen of Asp (nucleophile) on the carbon atom of the substrate, yielding a covalent alkyl-enzyme intermediate (**Fig. 4A**). The tetrahedral intermediate is stabilized by the amide nitrogens of halide-binding residues presented in the oxyanion pocket. The alkyl-enzyme intermediate is subsequently hydrolyzed by the water molecule activated by His (base). Catalytic acid stabilizes the charge developed on the imidazole ring of His (Damborsky & Koca, 1999) (**Fig. 4B**). Release of products is the last and slowest step in the catalytic cycle, which is largely determined by the size and affinity of the product alcohol (Bosma *et al.*, 2003; Janssen, 2004) (**Fig. 5**).

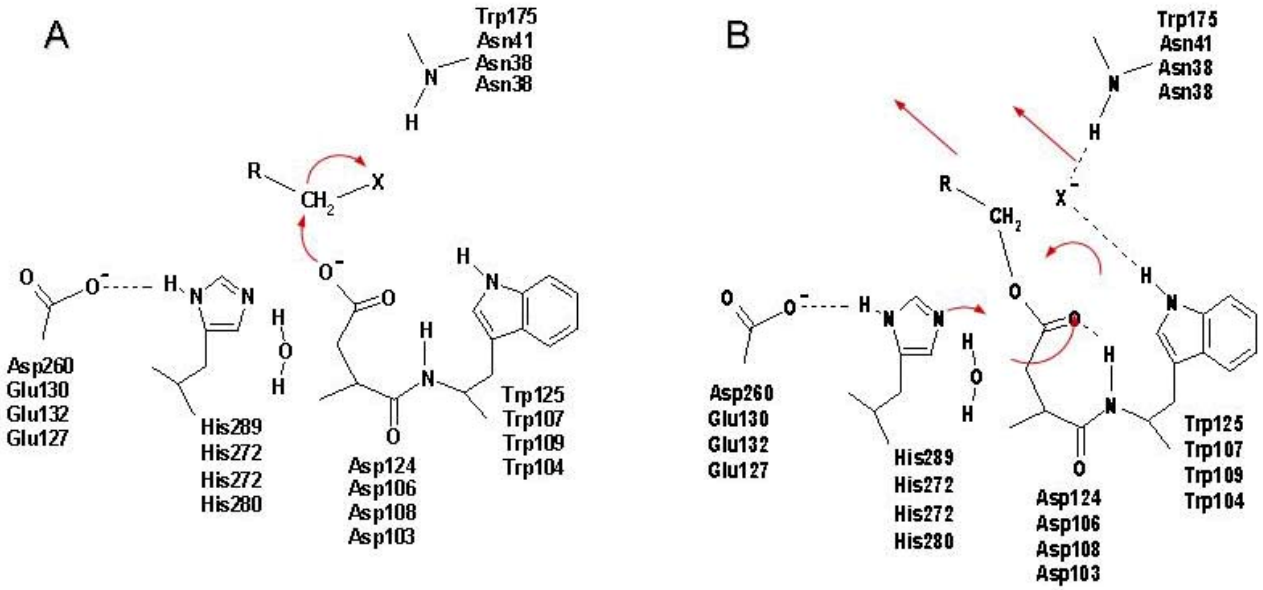

Figure 4. *General catalytic mechanism of haloalkane dehalogenases. (**A**) Formation of the covalent intermediate by S_N2 substitution. (**B**) Hydrolysis of the intermediate. Residue numbers refer to DhlA, DhaA, LinB, and DbjA, respectively (adapted from Janssen, 2004).*

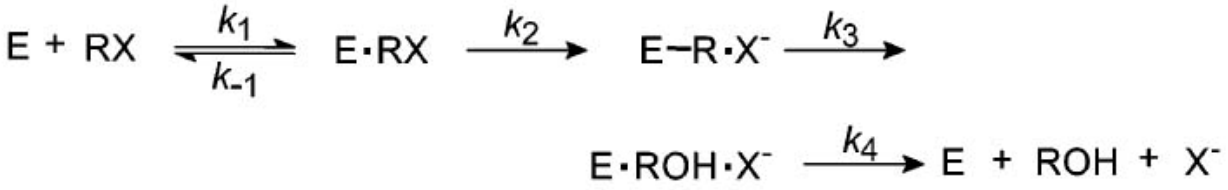

Figure 5. *Kinetic mechanism for haloalkane dehalogenases. The mechanism involves substrate binding, formation of an alkyl-enzyme intermediate and simultaneous cleavage of the carbon-halide bond, hydrolysis of the alkyl intermediate, and finally release of the products from the enzyme active site (adapted from Bosma et al., 2003).*

The wealth of knowledge that has been acquired about haloalkane dehalogenases in the past two decades makes these enzymes a good model system to study fundamental principles of enzymatic function (Klvana *et al*., 2009).

2.3. Applications of haloalkane dehalogenases

Carbon-halogen compounds are ubiquitous in the environment. Although a portion of these chemicals are generated by naturally occurring biotic and abiotic processes, the widespread use of halogen-based chemistry in industrial-scale

chemical processes has introduced many additional human-made halocarbons as solvents, degreasing agents, intermediates in chemical synthesis, and pesticides, into the environment (Swanson, 1999; Janssen & Schanstra, 1994). The cleavage of the carbon-halogen bonds in the halogenated compounds, which frequently represent environmental pollutants, is a key step in their decontamination (Janssen *et al*., 2005). Hence, the haloalkane dehalogenase enzymes can be used as biocatalysts in the environmental biotechnology (Pries *et al*., 1994b, Stucki & Thuer, 1995). Rapid progress has been made in the analysis of structure-function relationships in dehalogenases, by using X-ray crystallography, site-directed mutagenesis, kinetic analysis, quantum mechanics and molecular mechanics calculations, statistical analysis, and directed evolution (Janssen, 2004). Such complex analysis has opened the possibility of engineering enzymes with improved applicability in the detoxification of xenobiotic compounds (Janssen & Schanstra, 1994).

Moreover, haloalkane dehalogenases have been applied in industrial biocatalysis (Prokop *et al*., 2004) and also as active components of biosensors (Campbell *et. al*., 2006; Bidmanova *et al*., 2010). For example, haloalkane dehalogenases from *Rhodococcus* is presently developing for application in large-scale chemical processing (Swanson, 1994; Affholter *et. al*., 1998). Industrial biocatalysis may be conducted either with a whole-cell microbial catalyst or using an enzyme *ex vivo*. The microorganism or enzyme is frequently immobilized, improving enzyme stability and handling, and allowing maximum catalytic efficiency through a continuous process. Newer protein evolution technologies have a significant impact on the future industrial potential of these enzymes (Swanson, 1999).

Haloalkane dehalogenases also represent a good model system to study the structural basis of enantioselectivity (**Fig. 6**). The understanding of the molecular basis and thermodynamics of the enzymes enantioselectivity opens up new possibilities for constructing enantioselective biocatalysts by protein engineering. These enzymes could be used for the synthesis of pharmaceuticals, agrochemicals, and food additives (Prokop *et al.,* 2010).

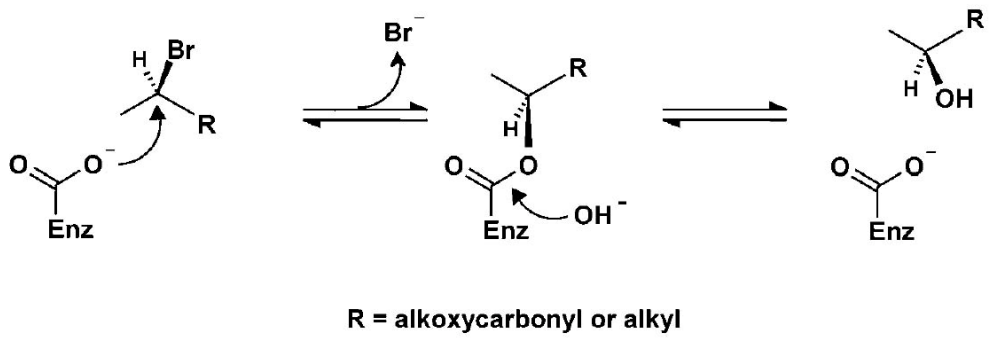

Figure 6. *Reaction mechanism of haloalkane dehalogenases with α-bromoesters and β-bromoalkanes (adapted from Prokop et al., 2010).*

Another promising area of haloalkane dehalogenases application is in decontamination of chemical warfare substances. A number of protective materials are being developed containing the enzymes for destruction of such substances and protection against chemical warfare agents (Prokop *et al*., 2005; Prokop *et al*., 2006).

2.4. Haloalkane dehalogenase DhaA from *Rhodococcus rhodochrous* NCIMB 13064

2.4.1. Structure and functions of DhaA enzyme

The haloalkane dehalogenase DhaA was isolated from Gram-positive soil bacterium *R. rhodochrous* NCIMB 13064 (Kulakova *et al*., 1997).

The DhaA protein is composed of the α/β-hydrolase core domain and the helical cap domain (**Fig. 7**). The core domain includes an eight-stranded β-sheet and 6 α-helices (β1-β2-β3-α1-β4-α2-β5-α3-β6, α8-β7-α9-β8-α10). The β-sheet is mostly parallel with a single antiparallel β-strand 2. The α/β-hydrolase domain forms a hydrophobic core that contains catalytic residues typical for haloalkane dehalogenases. The active site cavity is located between the core and cap domains. Asn41 is one of the pair of amino acids forming the halide-binding site and it is positioned in the loop joining β-strand 3 and α-helix 1. The nucleophile Asp106 and the halide-stabilizing Trp107 are located in the loop following β-strand 5. The catalytic base His272 is located in the loop between β-strand 8 and the C-terminal

α-helix 10. The acidic residue Glu130 is located in the loop following β-strand 6. The cap domain comprises of 5 α-helices (α4-α5'-α5-α6-α7) inserted between β-strand 6 and α-helix 8 of the α/β-hydrolase fold. The DhaA enzyme belongs to the HLD-II subfamily of haloalkane dehalogenase (Chovancova *et al.*, 2007; Newman *et al.*, 1999; Stsiapanava *et al.*, 2010).

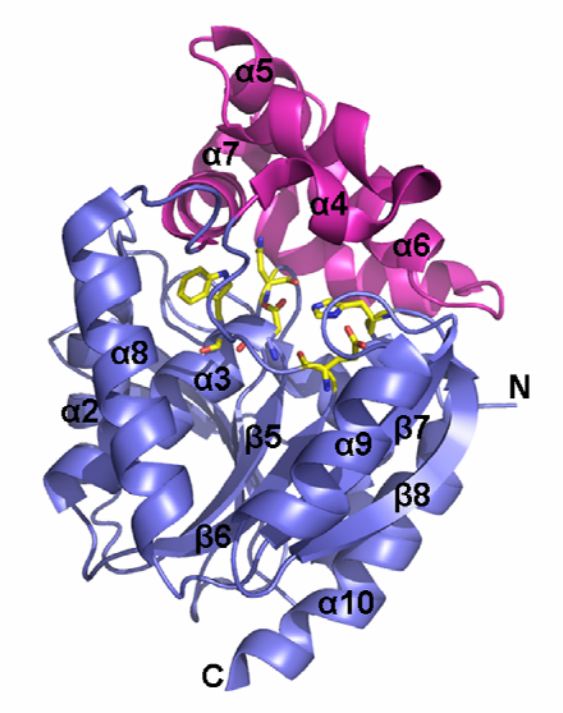

Figure 7. *Cartoon representation of the DhaA structure. The α/β-hydrolase core domain is shown in blue, the helical cap domain in magenta. Catalytic pentad residues are shown in yellow sticks representation (adapted from Stsiapanava et al., 2010).*

DhaA proteins have several tunnels that connect the active site cavity with bulk solvent and take part in exchange of ligands and solvent. The two major access tunnels are referred as the main tunnel and the slot tunnel (**Fig. 8A**). The main tunnel is located between α4 and α5 helices of the cap domain and is formed by nonpolar residues (such as Ala145, Phe144, Phe149, Phe168, Ala172, and Cys176), and polar residues as Thr148 and Lys175. The smaller side tunnel is found between α4 helix of the cap domain and loops connecting helix α4 with strand β3 of the core domain and strand β3 with helix α8. The side tunnel is surrounded by nonpolar amino acids Ile132, Ile135, Trp141, Pro142, Leu246 and Val245, and polar residues Arg133 and Glu140 (Otyepka & Damborsky, 2002;

Petrek *et al.*, 2006; Klvana *et al.*, 2009; Pavlova *et al.*, 2009; Stsiapanava *et al.*, 2010) (**Fig. 8B**).

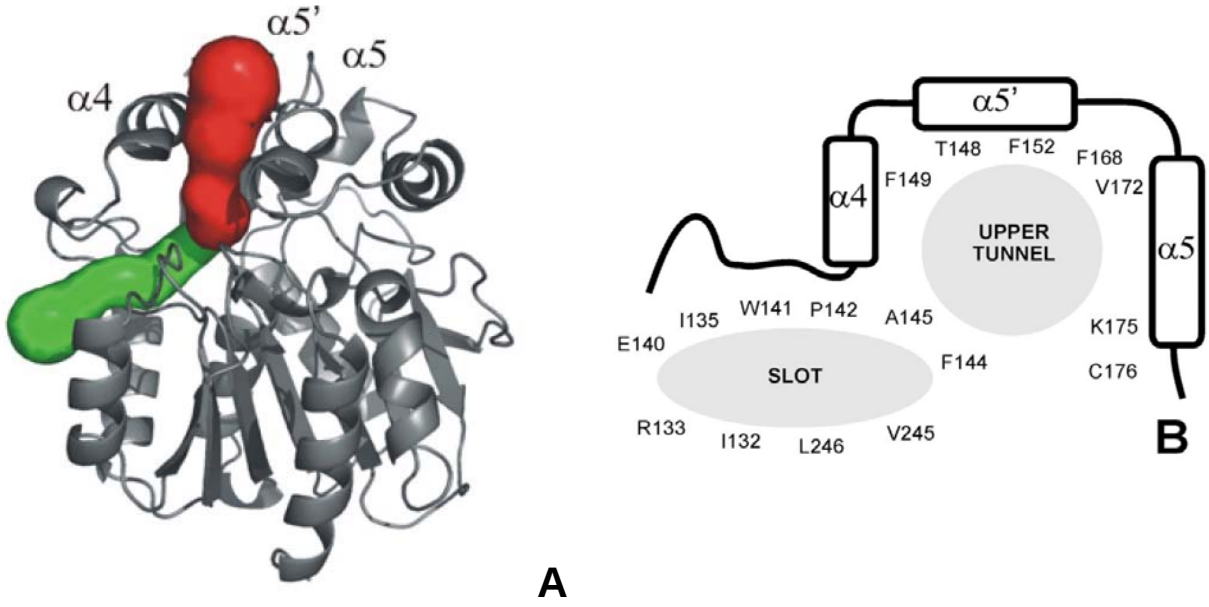

Figure 8. *DhaA tunnels. (**A**) Cartoon representation of the DhaA structure with tunnels found by CAVER. The main tunnel is colored in red. Slot is highlighted in green. (**B**) Schematic representation of access paths for DhaA identified by protein crystallography and molecular dynamic simulations (adapted from Petrek et al., 2006).*

DhaA is the most active on longer chain (C_2-C_8), cyclic, and multiply halogenated alkanes (Bosma *et al.*, 2002). In DhaA, halide release is a fast process, showing no effect on overall kinetics. The slowest step of haloalkanes conversion by the wild type DhaA lies at the beginning of the reaction cycle, before or in the step forming the halide ion product (Pavlova *et al.*, 2009).

Recently, DhaA has drawn interest because of its capacity to convert a highly toxic and persistent to chemical and biological degradation water pollutant and human carcinogen 1,2,3-trichloropropane (TCP) to 2,3-dichloropropane-1-ol (DCL) (**Fig. 9**). The efficiency of reaction is too low to use the wild type DhaA in biotechnological processes. Moreover, due to the low conversion rate, cells are longer exposed to toxic effects of TCP, which can inhibit their growth (Bosma *et al.*, 2002; Bosma *et al.*, 2003).

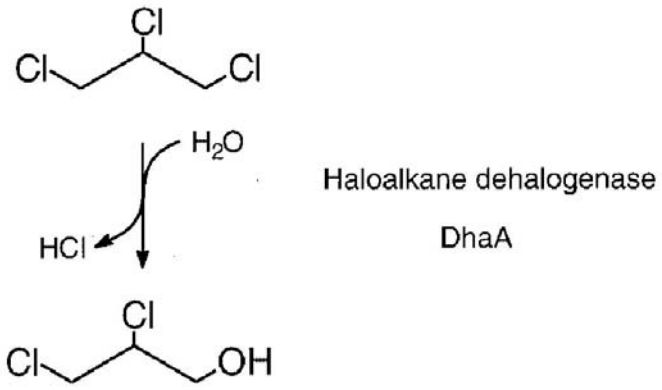

Figure 9. *DhaA involved conversion TCP to DCL (adapted from Bosma et al., 2002).*

2.4.2. DhaA protein variants

2.4.2.1. DhaA04, DhaA14 and DhaA15 variants

Protein engineering has been used for construction and evolution of modified DhaAs with improved catalytic properties towards TCP (Gray *et al*., 2001; Bosma *et al*., 2002; Pavlova *et al.*, 2009). The tunnel residues located outside of active site represent good targets for mutagenesis since their replacement does not lead to loss of functionality by disruption of the active site architecture (Pavlova *et al*., 2009). Bosma *et al.* (2002) reported a mutant selected by directed evolution and carrying substitution C176Y in the main tunnel. This mutant, named M1 by Bosma *et al.* (2002) and DhaA04 in our work, shows 3-fold improved catalytic efficiency with TCP compared to the wild-type enzyme. Banas *et al.* (2006) used molecular simulation to study the mechanism of improved catalysis of this mutant and proposed that the side-chain of the residue 176 narrows down the main tunnel, possibly making the side tunnel a preferred route in DhaA04. The mutant enzyme DhaA14, carrying mutation I135F in the side tunnel, was constructed by site-directed mutagenesis to reveal the importance of the side tunnel for catalysis. DhaA15 carries both mutations (C176Y+I135F) in the main tunnel and the side tunnel (**Fig. 10**).

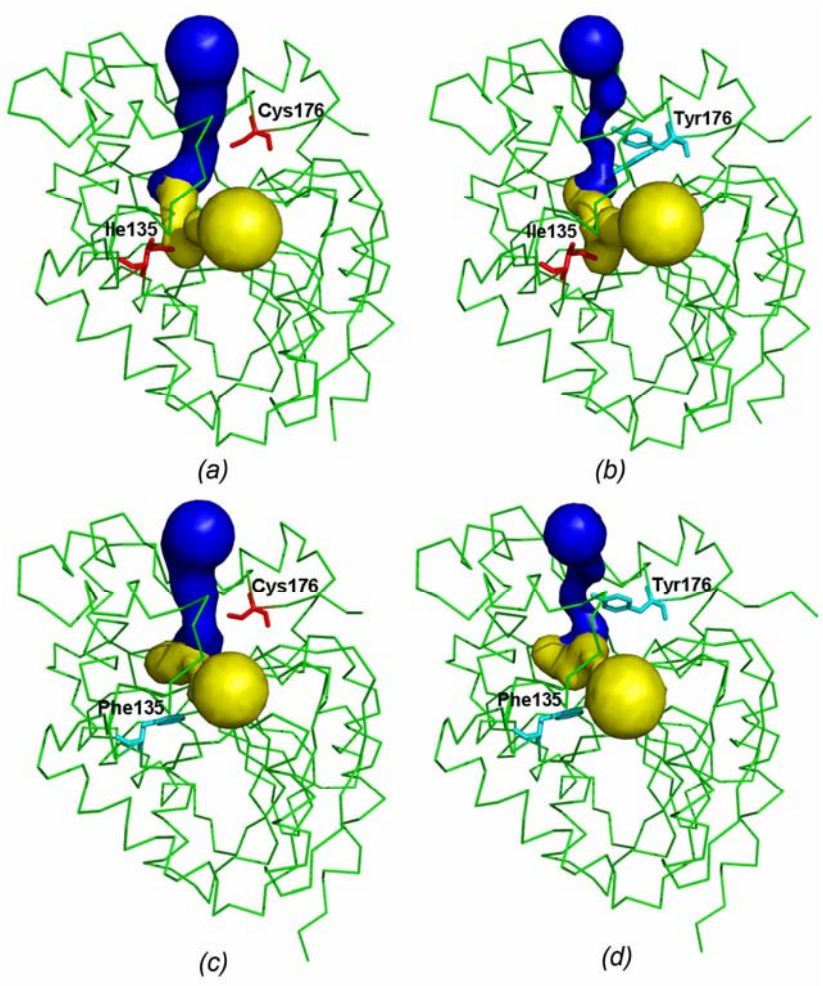

Figure 10. *Ribbon representations of structures of wild type DhaA (a), DhaA04 (b), DhaA14 (c), DhaA15 (d) with the main tunnel (in blue) and the side tunnel (in yellow). The residues selected for mutagenesis are shown in red sticks; the mutated residues are represented by cyan sticks (adapted from Stsiapanava et al., 2010).*

All constructed proteins were characterized for 1. their activity with TCP using steady-state kinetics and for 2. proper folding by circular dichroism (CD) spectroscopy. DhaA04 and DhaA15 mutants showed an increase in the rate of TCP conversion. The Michaelis constants determined for the mutants with TCP were similar to those for wild type DhaA in all variants (**Table 1**) (Klvana *et al*., 2009).

Table 1. W*ild type DhaA, its mutants and their kinetic parameters for TCP conversion (adapted from Klvana et al., 2009).*

	Variable residues		K_m[a] (mM)	k_{cat}[a] (s^{-1})	k_{cat}/K_m ($s^{-1} M^{-1}$)
	Main tunnel	Slot tunnel			
DhaA	176	135			
WT	C	I	1.0 (±0.2)	0.04 (±0.01)	40
04	Y	I	1.7 (±0.1)	0.24 (±0.01)	141
14	C	F	1.5 (±0.3)	0.05 (±0.02)	33
15	Y	F	1.8 (±0.2)	0.23 (±0.01)	128

The same level of K_m of the wild type enzyme and the mutants corresponds with the fact that the residues targeted by mutagenesis are localized in the access tunnels rather than in the active site. Mutants 04, 14 and 15 showed a similar intensity of their CD spectra to wild type DhaA, confirming that the secondary structure of these enzymes was not significantly affected by the introduced mutations (Klvana *et al*., 2009).

2.4.2.2. DhaA13 protein variant

DhaA13 protein variant, carrying mutation H272F in the catalytic histidine, was prepared to catch the protein in a complex with alkyl-enzyme intermediate. This mutant variant binds substrate to the active site, catalyses the first reaction step leading to the formation of the alkyl-enzyme intermediate (**Fig. 11A**) that is not able to convert it further to the product (**Fig. 11B**) (Jesenska *et al*., 2009).

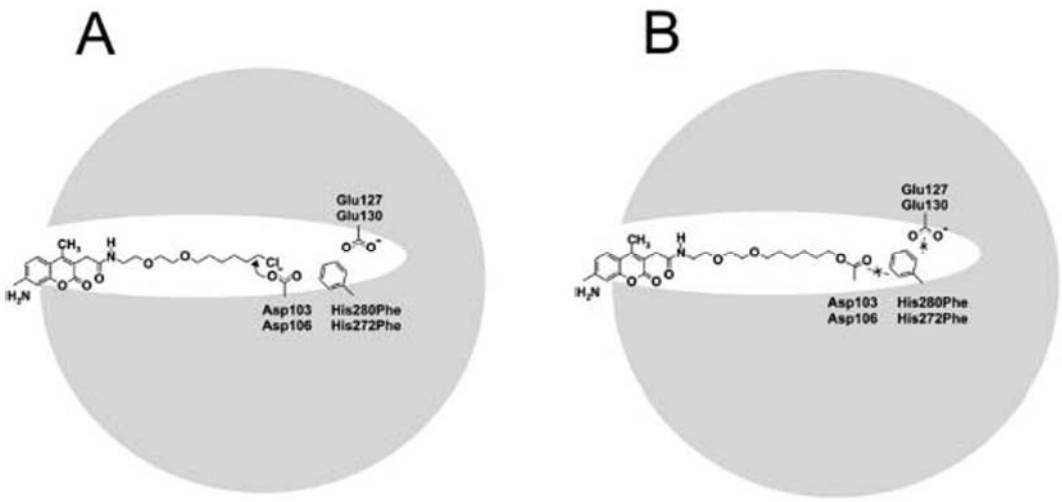

Figure 11. *Schematic representation of the formation of the covalent ligand-protein complex between the DhaA13 mutant and the dye coumarine (**A** and **B**) (adapted from Jesenska et al., 2009).*

3. Experimental methods

X-ray diffraction analysis is the most common experimental method allowing the construction of detailed models of large molecules by interpretation the X-ray diffraction patterns, which arise from many identical molecules in an ordered array called a *crystal*.

3.1. Crystallization of biological macromolecules and crystal structure determination

Visible light is electromagnetic radiation with wavelengths of 400-800 nm. This light does not produce an image of individual atoms in protein molecules, in which bonded atoms are only about 0.15 nm (or 1.5 angstroms) apart from each other. In order to achieve this, electromagnetic radiation of a wavelength falling into the X-ray range has to be used. However, the scattering of X-rays from a single protein or nucleic acid molecule would be almost immeasurable. Consequently, a large number of such molecules have to be organized into an array, so that their scattering contributions are constructive. Then, the resultant radiation can be observed and quantitated as a function of direction in space. This is precisely what *macromolecular crystals* provide. They are precisely ordered, making the three-dimensional arrays of molecules, and helding together by non-covalent interactions. The crystal can be developed as a three-dimensional form composed from basic building blocks – the *asymmetric units*. The asymmetric unit is the smallest portion of a crystal structure to which symmetry operations can be applied in order to generate the complete *unit cell* (the crystal repeating unit) (**Fig. 12**). The unit cell is the smallest and simplest volume element that is completely representative of the whole crystal. The most common symmetry operations for crystals of biological macromolecules are rotations, translations and screw axes (combinations of rotation and translation). Application of crystallographic symmetry operations to an asymmetric unit yields one unit cell that when translated in three dimensions makes up the entire crystal (McPherson, 2002; Rhodes, 2006; http://www.pdb.org).

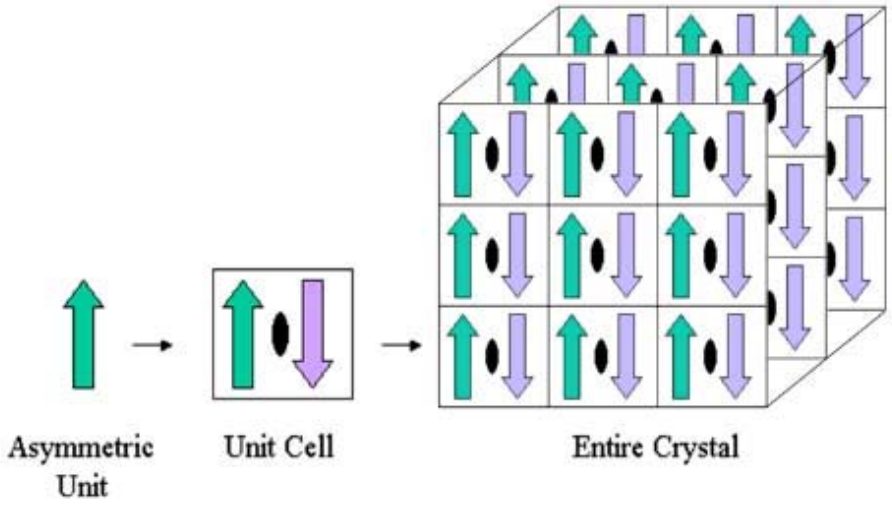

Figure 12. *Creation of a crystal from a fundamental asymmetric unit (adapted from http://www.pdb.org).*

The asymmetric unit contains the unique part of a crystal structure. It is used by the crystallographer to refine the coordinates of the structure against the experimental data and may not necessarily represent a whole biologically functional assembly (http:// www.pdb.org).

3.1.1. Macromolecular crystallization

3.1.1.1. Basic of method

The first protein crystals, crystals of hemoglobin, were grown over 150 years ago and these were recognized as a link between the living and the inanimate world. Since then, protein crystals have evolved from objects of demonstration of molecular purity to essential intermediates in the discovery of macromolecular structure. During the course of that, evolution methods of crystallization developed from empirical, trial and error approaches to the physical characterization concepts (Bergfors, 1999).

Crystal formation (aggregation) occurs in two stages, as a nucleation, and a growth (**Fig. 13A**). To promote either stage, a condition of supersaturation must be created in the crystallization medium. In the first stage, molecules must overcome an energy barrier to form a periodically ordered aggregate of critical size. Nucleation requires protein and/or precipitant concentrations higher than those

optimal for slow precipitation. The second step, growth, is achieved by making solid state more attractive to individual molecules than the free, solution state. Slow precipitation is more likely to produce lager crystals, whereas rapid precipitation may produce many small crystals, or an amorphous solid. An ideal strategy (**Fig. 13B**) would be to start with conditions corresponding to the labile zone of the phase diagram, and then, when nuclei form, move into the metastable zone, where growth, but not additional nucleation, can occur (McPherson, 1999; Rhodes, 2006).

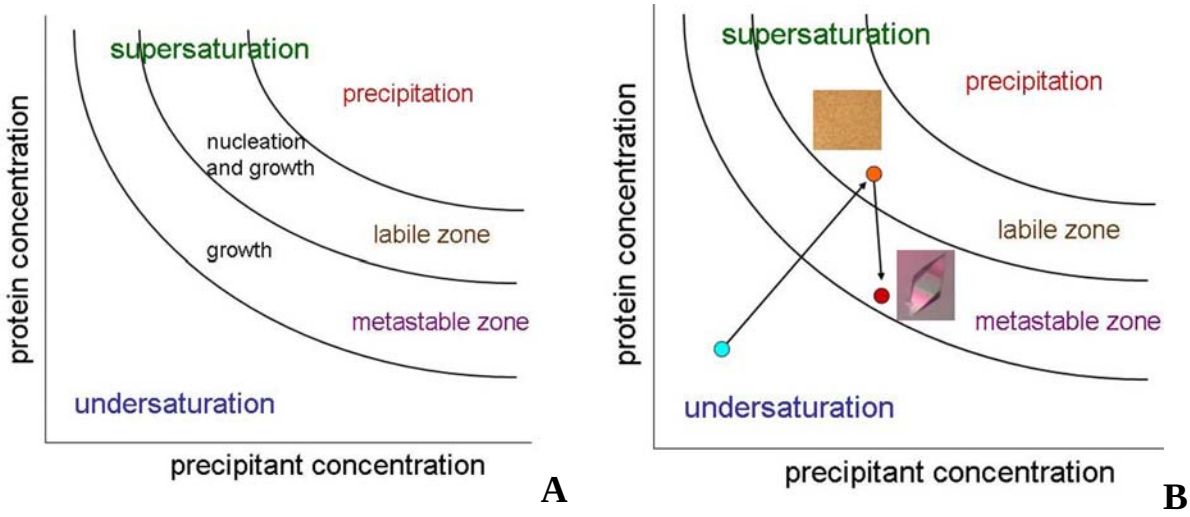

Figure 13. *(**A**) Phase diagram for crystallization mediated by a precipitant. (**B**) An ideal strategy for growing large crystals.*

3.1.1.2. Crystallization techniques

Nowadays several methods based on brining the solution of macromolecules to the supersaturation state exist: vapor diffusion methods, batch, microbatch under oil, microdialysis or counter diffusion. The most frequently used crystallization method is the *vapor diffusion technique*, in which the protein/precipitant solution is allowed to equilibrate in a closed container with a larger aqueous reservoir whose precipitant concentration is optimal for producing crystals. In this technique a small droplet (1-10 µl) of the protein is mixed with an equal or similar volume of the crystallization solution. In the case of the hanging-drop method (**Fig. 14A**), a mixed droplet is placed on a glass cover slip, which is sealed onto the top of the

reservoir with grease. In the sitting-drop technique (**Fig. 14B**), droplets of the sample mixed with crystallization reagent are placed on a platform over a reservoir. A third method, in which the droplet is simultaneously in contact with both an upper and lower surface, is called a sandwich-drop (**Fig. 14C**). The difference in concentration between the drop and the reservoir drives the system toward equilibrium by diffusion through the vapor phase. In a perfectly designed experiment, the protein becomes supersaturated and crystals start to form when the drop and reservoir are at or close to equilibrium (McPherson, 1999; Bergfors, 1999; Rhodes, 2006).

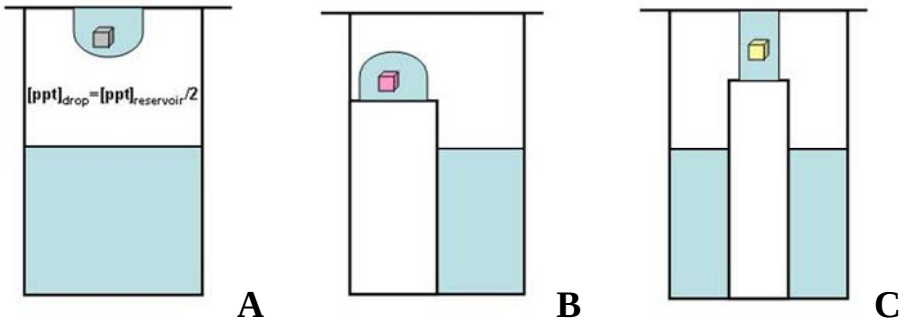

Figure 14. *Schematic representation of vapor diffusion techniques: (**A**) hanging-drop, (**B**) sitting-drop, (**C**) sandwich-drop.*

Sometimes many small crystals grow instead of a few that are large enough for diffraction measurements. Small crystals of good quality can be used as a seeds to grow larger crystals. The experimental setup is the same as before, except that each droplet is seeded with one or a few small crystals. Seeds may also be obtained by crushing small crystals or crystal clusters. Crystals may grow from seeds up to ten times faster than they grow anew; so most of the dissolved protein goes into only a few crystals (Rhodes, 2006).

3.1.1.3. Finding optimal conditions for crystal growth

Many variables and parameters influence the formation of macromolecular crystals. These include e.g. protein purity, concentrations of protein and precipitant, pH, and temperature, as well as vibration and sound, convection, source and age of protein, and the presence of ligands. Because each protein is

unique, it is difficult to predict the specific values of a variable, precipitation points, or sets of conditions that could be used to produce suitable diffraction quality crystals. The specific components and conditions must be carefully identified and refined for each protein. The difficulty and importance of obtaining good quality crystals has prompted the development of crystallization robots that are programmed to set up many trials under systematically varied conditions.

When varying the more conventional parameters fails to produce good crystals limited digestion of protein may be applied. In this method, a proteolytic enzyme removes a disordered surface loop, resulting in a more rigid, hydrophilic, or compact molecule that forms better crystals. The protein-ligand complexes may be more likely to crystallize compared with the free protein, either because the complex is more rigid than the free protein or because the ligand induces a conformational change that makes the protein more amenable to crystallization. Membrane proteins are different from soluble proteins in that respect as they are greatly under-represented in the Protein Data Bank (PDB; Berman *et al*., 2000), due to their resistance to crystallization. These proteins have sometimes been crystallized in the presence of detergents, which coat the hydrophobic portions and decorate it with polar or ionic groups, thus rendering it more soluble in water. A number of membrane proteins have been diffused into semi-crystalline phases of lipid to produce ordered arrays that diffracted well and yielded protein structures (McPherson, 1999; Rhodes, 2006).

Once the suitable crystals have been grown, the planning of data collection strategy can be done.

3.1.2. Crystal structure determination

3.1.2.1. Crystallographic data collection

The diffraction experiment involves: 1. the generation of X-rays, 2. the selection of X-rays for specific experiment, 3. the preparation of the crystal for the experiment, 4. the actual data collection step, and 5. the processing and validation

of the resulting data. The quality of a crystal structure is directly determined by the quality of the diffraction data that are the basis for the determination of the protein structure (Wilmanns & Weiss, 2005).

In a diffraction experiment a collimated beam of monochromatic X-rays is directed through an object and rays are scattered in all directions by the electrons of every atom in the object with a magnitude proportional to the size of its electron complement (**Fig. 15**). The electrons surrounding the nuclei of the atoms in the crystal scatter the X-rays, which subsequently interfere with one another to produce the diffraction pattern on the film or electronic detector face. Each atom in the crystal serves as a center for scattering of the waves, which then form the diffraction pattern. The magnitudes and phases of the waves contributed by each atom to the interference pattern (the diffraction pattern) is strictly a function of each atom's atomic number and its position (***x, y, z***) relative to all other atoms. The objective of an X-ray diffraction analysis is to extract that information and determine the relative atomic positions (McPherson, 2003).

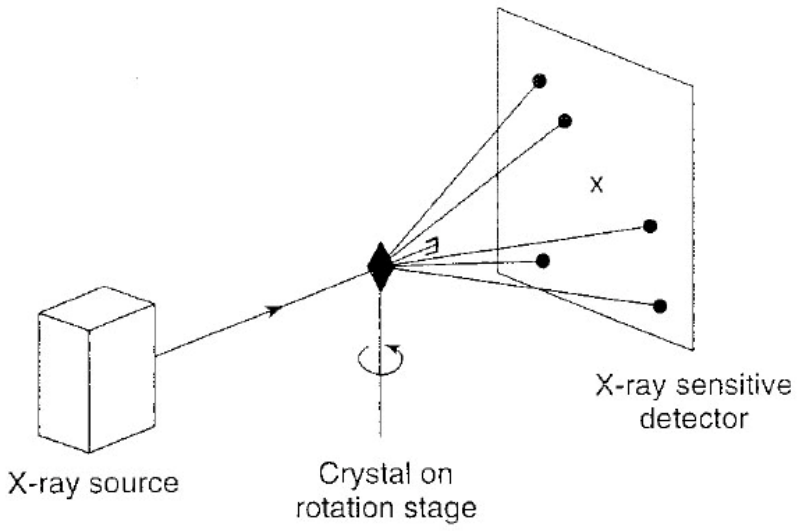

Figure 15. *Schematic representation of the diffraction experiment (adapted from Wilmanns & Weiss, 2005).*

The complete diffraction pattern from a protein crystal is not limited to a single planar array of intensities. Each diffraction frame corresponds to only a limited set of orientations of the crystal with respect to the X-ray beam. In order to record the

entire three-dimensional X-ray diffraction pattern, a crystal must be aligned with respect to the X-ray beam in all orientations. From many two-dimensional arrays of reflections, corresponding to cross-sections through diffraction space, the entire three-dimensional diffraction pattern composed of tens to hundreds of thousands of reflections is compiled (McPherson, 2003).

3.1.2.2. Scattering by a crystal

In order to build up a crystal from its smallest unit, unit cell, it is necessarily to know the contents of the unit cell and the lattice translations ***a***, ***b***, and ***c***. For describing the scattering of one single unit cell of a crystal, $\boldsymbol{F}_{\text{unit cell}}(\boldsymbol{s})$, the contributions of all ***N*** atoms in the unit cell have to be added up (eqn [1]):

$$\boldsymbol{F}_{\text{unit cell}}(\boldsymbol{s}) = \sum_{j=1}^{N} f_j(\boldsymbol{s}) \mathrm{e}^{2\pi \mathrm{i} \boldsymbol{r}j \cdot \boldsymbol{s}} \qquad [1]$$

where ***s*** is the scattering vector describing the change in direction in that the X-ray wave undergoes upon scattering. $f_j(\boldsymbol{s})$ is the atomic form factor that presents total wave scattered by object and $\boldsymbol{r}_j$ is the coordinates of the atoms ***j***.

In order to consider the scattering by the whole crystal, the contributions of all unit cells of the crystal and all atoms in each unit cell have to be taken into account. Consequently, to describe the scattering by the whole crystal, it is sufficient to consider the scattering by just one unit cell (eqn [2]):

$$\boldsymbol{F}_{\text{crystal}}(\boldsymbol{s}) = \boldsymbol{n}\boldsymbol{F}_{\text{unit cell}}(\boldsymbol{s}) = \boldsymbol{n} \sum_{j=1}^{N} f_j(\boldsymbol{s}) \mathrm{e}^{2\pi \mathrm{i} \boldsymbol{r}j \cdot \boldsymbol{s}} \qquad [2]$$

where ***n*** is the number of unit cells (Wilmanns & Weiss, 2005).

In any particular direction, the radiation scattered by the row of points will have zero intensity by destructive interference of the individual scattered rays unless these are all in phase (Clegg, 1998). Only in those directions ***s***, in which the rays are in phase, scattering will be observed. In all other directions the sum of all scattered waves will be zero. This leads to the observation of a diffraction pattern

consisting of discrete maxima, the so-called X-ray reflections. Each reflection is identified by a unique combination of the three numbers ***h, k,*** and ***l***, named Miller indices. With these indices equation [2] can be transformed into the "structure factor equation" [3]:

$$\boldsymbol{F(s)} = \boldsymbol{F(hkl)} = \sum_{j=1}^{N} f_j \, \mathrm{e}^{2\pi \mathrm{i}(hxj+kyj+lzj)} \qquad [3]$$

Together with the "electron density equation" [4], it constitutes one of the two central equations in the X-ray crystallography. It describes the scattering of a crystal defined by the unit cell vectors ***a, b***, and ***c***, and by the atoms inside the unit cells of this crystal as defined by the atomic form factors (f_j) and the fractional coordinates (x_j, y_j, and z_j).

3.1.2.3. The electron density equation and solving the phase problem

The electron density equation (eqn [4]) is the second important equation in crystallography:

$$\rho(\boldsymbol{r}) = \int_{\mathrm{Vol}^*} f_j(\boldsymbol{s}) \mathrm{e}^{-2\pi \mathrm{i} \boldsymbol{r}\cdot\boldsymbol{s}} \mathrm{d}V^* \qquad [4]$$

Instead of integrating over the volume of the scattering object V, the integration proceeds over diffraction space, which is also called reciprocal space, because of reciprocal relationship to the real space with respect to its geometric parameters.

In order to calculate the value for the electron density $\boldsymbol{\rho}$ at any given point (***x, y, z***), all reflections should be taken into account. The summation can only be carried out if both the structure factor amplitude l***F***l and the phase $\boldsymbol{\alpha}$ are known for each reflection (***hkl***) [5]:

$$\rho(x, y, z) = \frac{1}{\mathrm{V}} \sum_{h,k,l} |F(hkl)| \mathrm{e}^{-2\pi \mathrm{i}(hx+ky+lz)+\mathrm{i}\alpha(hkl)} \qquad [5]$$

where **V** is the volume of unit cell (Wilmanns & Weiss, 2005).

The amplitude of $|F_{(hkl)}|$ is proportional to the square root of the reflection intensity $I_{(hkl)}$, so structure-factor amplitudes are directly obtainable from measured reflection intensities. In order to compute $\rho(x, y, z)$ from the structure factor, in addition to the intensity of each reflection, the phase $\alpha_{(hkl)}$ of each diffracted ray must be obtained. But the phase is not directly obtained from a single measurement of the reflection intensity. This is known as the so-called "phase problem" in crystallography. The phase problem is the reason why an image of the studied molecule cannot be calculated directly from the diffraction data. Over time, a number of methods have been developed to circumvent the phase problem. Today, the most common methods are ***isomorphous replacement, anomalous scattering***, and ***molecular replacement*** (Rhodes, 2006; Wilmanns & Weiss, 2005).

3.1.2.3.1. Isomorphous replacement

In this method, diffraction data sets of two isomorphous crystals are compared with each other reflection by reflection. The first crystal may be the one of the native macromolecules, the second crystal may be the one of a heavy atom derivative of the same macromolecule. The latter can be prepared by either co-crystallization or soaking a native macromolecule crystal in a heavy atom-containing solution. In many cases, such ions are bounded to one or a few specific sites on the protein without perturbing its conformation or crystal packing. A detailed comparison of the two diffraction data sets will then yield the differences between the data sets, which are due to the heavy-atom substructure. From these differences the substructure can be determined. With the substructure at hand, the structure factor amplitude and the phase of just the substructure can be calculated, and then use this heavy-atom phase as a reference to calculate the phases of the reflections of the macromolecule crystal.

The vector addition of the structure factor of the macromolecule F_P and the structure factor of the heavy atoms F_H will yield the structure factor of the heavy-atom derivative F_{PH} (**Fig. 16**). If the magnitudes of both F_P and F_{PH} (these are the structure factor amplitudes, which have been measured in the two diffraction

experiments) and the magnitude and direction of $\boldsymbol{F}_H$ (this can be calculated once the heavy-atom substructure is known) are known, all other parameters of the triangle can be calculated.

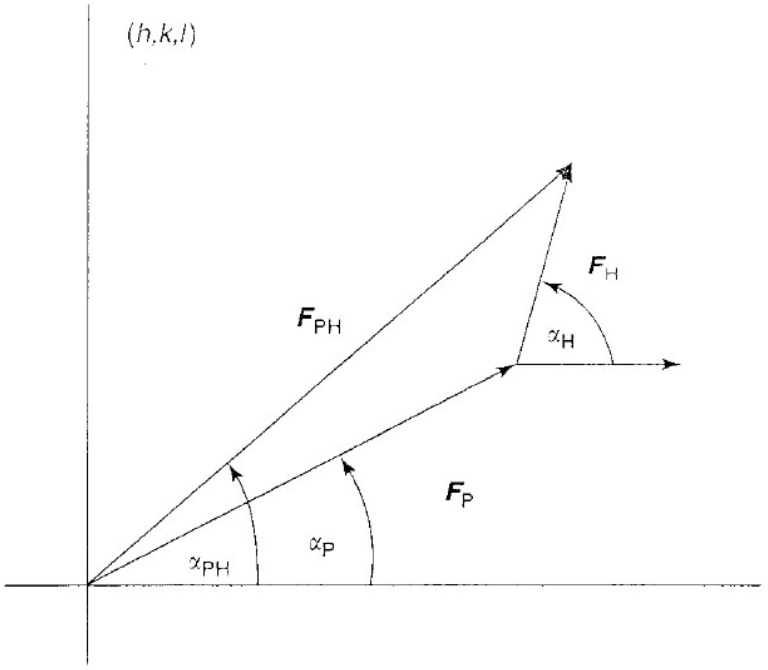

Figure 16. *Vector addition of the structure factors for the native macromolecule* $\boldsymbol{F}_P$ *, the heavy-atoms substructure* $\boldsymbol{F}_H$*, and the heavy-atom derivative of the macromolecule* $\boldsymbol{F}_{PH}$ *(adapted from Wilmanns & Weiss, 2005).*

However, the result of this calculation will not be a unique phase $\boldsymbol{\alpha}_{(hkl)}$ for the given reflection, but two possible solutions, which are symmetrical about the vector $\boldsymbol{F}_H$. This situation can be made unambiguous by including a second heavy-atom derivative (Wilmanns & Weiss, 2005; Rhodes, 2006) or anomalous scattering (see next paragraph).

3.1.2.3.2. Anomalous diffraction

If the structure to be determined contains anomalous scatterers (anomalous scattering occurs when the energy of the X-rays used for the diffraction experiment is close to an energy that is absorbed by an atom), a diffraction experiment can be carried out at two (or more) different X-ray energies. The anomalous scattering

atoms may be 1. selenium in selenomethionines, 2. atoms that occur naturally in the macromolecules, or 3. heavy atoms introduced into the crystal by soaking or co-crystallization. The differences between the diffraction patterns can be then again attributed to the anomalously scattering substructure, and in the same way as above, the substructure can be determined, and the substructure phase be used as a reference to determine the phase $\boldsymbol{\alpha}_{(hkl).}$ Anomalous diffraction yields particularly good phase information at high resolution (Wilmanns & Weiss, 2005; McPherson, 2003).

3.1.2.3.3. Molecular replacement

In the case, if the structure to be determined is expected to be similar to another structure that is known already, the known structure can be placed in the unit cell of the structure to be determined, and the structure factor $\boldsymbol{F}_{\mathrm{P}}$ calculated. The phase $\boldsymbol{\alpha}_{(hkl)}$ of the structure factor amplitude $|\boldsymbol{F}_{\mathrm{P}}|$ will be approximately correct and can be used as a starting value for further refinement. The initial step in the determination of the molecular replacement structure is the determination of three rotation and three translation parameters, which define the correct orientation and the correct translation of the search model (the known structure) in the unit cell of the target structure (the structure to be determined) (Wilmanns & Weiss, 2005).

Currently about two thirds of all newly characterized structures are determined by molecular replacement (Long *et al*., 2007). As more macromolecular structures become known through X-ray crystallography, molecular replacement method will have greater and greater application (McPherson, 2003).

3.1.2.4. Model building and refinement

Once initial phases have been determined by one of the methods described above, the electron density can be calculated according to eqn [5]. The electron density shows, where are the electrons (i.e., the atoms) in the unit cell. Since molecular structures are usually described by the position of all of their atoms, the electron density should be interpreted in terms of atomic positions and identities. Finally,

the model thus obtained can be subjected to a mathematical optimization procedure called refinement, in order to optimize the fit between the structure factors that can be calculated from the model and the structure factors that have been observed experimentally (Wilmanns & Weiss, 2005). The progress of refinement is typically monitored by looking at the R-factor (eqn [6]):

$$R = \sum ||F_{obs}| - |F_{calc}|| / \sum |F_{obs}| \qquad [6]$$

However, the problem with the R-factor is that it will automatically decrease as more parameters are introduced into the model. Therefore, Brünger (1992) suggested introducing the so-called **free R-factor**. For the free R-factor a small percentage of the reflections (less than 10%) are set aside for refinement and are solely used for monitoring the refinement progress. With the use of the free R-factor problems such as over-fitting the data have virtually disappeared.

4. Summary of papers

The **paper I** is focused on the crystallization and preliminary diffraction analysis of three DhaA mutants. The enzyme DhaA from *Rhodococcus rhodochrous* NCIMB 13064 belongs to the haloalkane dehalogenases which catalyze hydrolysis of haloalkanes to corresponding alcohols. Besides a wide range of haloalkanes, DhaA can slowly convert serious industrial pollutant 1,2,3-trichloropropane (TCP). The DhaA protein is expected to have several pathways (tunnels) connecting buried active site with surrounding solvent. Derived mutant enzymes DhaA04 and DhaA14 with mutations introduced to the residues located in two different tunnels were constructed to reveal importance of these tunnels for enzymatic activity with TCP. Mutant enzyme DhaA15 carries both mutations at the same time. Crystals of three mutants in the efficient quality for diffraction experiments were grown using a sitting-drop vapor-diffusion method. These crystals were used for X-ray diffraction experiments that were done at the beamline X11 of a DORIS storage ring at the EMBL Hamburg Outstation. Crystals of DhaA04, DhaA14 and DhaA15 mutants diffracted to the high resolutions of 1.3 Å, 0.95 Å and 1.15 Å, respectively. Crystal of DhaA04 protein belonged to the orthorhombic space group $P2_12_12_1$ while crystals of second two enzymes DhaA14 and DhaA15 to the triclinic space group $P1$. The known structure of the haloalkane dehalogenase from *Rhodococcus* species (PDB code 1BN6), renumbered according to gene sequence, was used as a template for the molecular replacement.

Pathways and mechanisms for product release in eight mutants of DhaA haloalkane dehalogenase carrying mutations at the residues lining two tunnels were explored using classical and random acceleration molecular dynamics simulations and the results were described in the **paper II**. The mutants showed distinct catalytic efficiencies with the halogenated substrate 1,2,3-trichloropropane. From the study of the mutants five different pathways denoted p1, p2a, p2b, p2c, and p3, were identified. Two out of the five pathways (p1 and p2a) were observable in the crystal structures, while all the three other pathways were identified by molecular

dynamics simulations. The individual pathways showed differing selectivity for the products: the chloride ion releases solely through p1, whereas the alcohol releases through all five pathways. Water molecules played a crucial role for release of both products by breakage of their hydrogen-bonding interactions with the active-site residues and shielding the charged chloride ion during its passage through a hydrophobic tunnel. It was concluded that the ligands could be exchanged between the buried active site and the bulk solvent through a permanent tunnel, passage through a transient tunnel, and passage through a protein matrix. It was demonstrated that the accessibility of the pathways and the mechanisms of ligand exchange were modified by mutations. Insertion of bulky aromatic residues in the tunnel corresponding to pathway p1 leaded to reduced accessibility to the ligands and a change in mechanism of opening from permanent to transient. It was proposed that engineering the accessibility of tunnels and the mechanisms of ligand exchange was a powerful strategy for modification of the functional properties of enzymes with buried active sites.

The structures of three haloalkane dehalogenase mutants are analyzed and compared in the **paper III**. The crystal structures of DhaA04 (C176Y), DhaA14 (I135F) and DhaA15 (C176Y+I135F) were solved by the molecular replacement method at the resolutions of 1.23 Å, 0.95 Å and 1.22 Å, respectively. The active site of DhaA04 contained a molecule of a ligand best represented by benzoic acid, with unknown origin. The isopropanol molecule detected in the structures of DhaA14 and DhaA15 entered the active site of these mutants from the crystallization solution. No water molecules are observed in the presence of benzoic acid or isopropanol. In the absence of these ligands, three and one water molecules fill the empty space in the active site of DhaA04 and DhaA14, respectively. In the case of the active site of DhaA15, no electron density for water molecules was observed. The position of the chloride ion in the active site was approximately the same in all the three described structures. The point mutations in the DhaA04, DhaA14 and DhaA15 proteins led to changes of anatomy of the main

tunnel, side tunnel and both the main tunnel and the side tunnel, respectively. The substitution of Cys176 by Tyr in the DhaA04 and DhaA15 mutants partially blocked the main tunnel when the active site was occupied by benzoic acid or isopropanol. At the same time, the side chain of Tyr176 could change conformations controlling exchange of these ligands. The side-chain of mutated Phe135 in DhaA14 and DhaA15 was modeled in one conformation and most probably did not have the opportunity to change its position. It was found that the bulky side chain of Phe135 almost completely blocks the small side tunnel in the mutated enzymes, suggesting that the main tunnel may still be the major pathway for the exchange of ligands in DhaA mutants.

In the **paper IV**, the crystallization and initial X-ray diffraction characterization of wild type DhaA and its variant DhaA13 in complex with the environmental pollutant trichloropropane (TCP) are reported. Further, the crystallization of DhaA13 in complex with the fluorescence dye coumarin was described. The complex with coumarin specifically located in the tunnel mouth of the DhaA13 enzyme was used in time-resolved fluorescence spectroscopy to monitor hydration, accessibility and mobility of the dye and its microenvironment in the protein. Finally, we described the complexes of the wild type DhaA with two different concentrations of isopropanol to investigate ability of this ligand to access into the enzyme active site and the effect on enzyme structure. All crystallization experiments were performed using the sitting-drop vapour-diffusion method. Diffraction data for wild type DhaA crystal grown from the solution containing 6% (*v/v*) isopropanol was measured at a home diffractometer (Institute of Molecular Genetics, Prague). This crystal diffracted to the resolution of 1.70 Å and belonged to the triclinic space group *P*1. Diffraction data for wild type DhaA crystal grown from the solution with 11% (*v/v*) isopropanol, for DhaA13 crystal soaked with TCP for three hours and for DhaA13 in complex with dye coumarin were collected at the EMBL/DESY in Hamburg. The crystals diffracted to a maximal resolution of 1.26 Å, 1.60 Å and 1.33 Å, respectively. The crystals of wild type DhaA and

variant DhaA13 in complex with dye coumarin belonged to the triclinic space group *P*1 while the crystal of DhaA13 complexed with TCP belonged to the orthorhombic space group $P2_12_12_1$. Data collections for wild type DhaA crystal grown in the presence of TCP in the crystallization solution and for DhaA13 crystal soaked with TCP for 40 hours were carried at BESSY II in Berlin. The crystals diffracted to maximal resolutions of 1.04 Å and 0.97 Å, respectively. Both crystals belonged to the triclinic space group *P*1. The structures of wild type DhaA and variant DhaA13 were solved by molecular replacement using the coordinates from *R. rhodochrous* haloalkane dehalogenase (PDB code 3FBW) as a search model.

Crystallization and crystallographic analysis of the mutant DhaA31 and its complex with 1,2,3-trichloropropane (TCP) is described in the **paper V**. Wild type DhaA can very slowly convert toxic non-natural compound and human carcinogen 1,2,3-trichloropropane to 2,3-dichloropane-1-ol. To increase the efficiency of this reaction the mutant DhaA31 with up to 32-fold higher catalytic activity than parent wild type enzyme was constructed. The DhaA31 was crystallized by sitting drop vapour-diffusion technique and crystals of DhaA31 in a complex with TCP were obtained using soaking experiment. Single crystals of DhaA31 and DhaA31 in the complex with TCP were used for X-ray diffraction measurements at EMBL Hamburg Outstation**.** Diffraction data for DhaA31 and DhaA31 with TCP were collected to high resolutions of 1.31 Å and Å 1.26 Å, respectively. The crystals belonged to the triclinic space group *P*1. The structures of DhaA31 and its complex with TCP were solved by the molecular-replacement method using the structure of haloalkane dehalogenase DhaA from *R. rhodochrous* (PDB ID code 3FBW).

References

Affholter, J. A., Swanson, P. E., Kan, H. L., Richard, R. A. (1998). World Patent 9836 080.

Bergfors, T. M. (1999). *Protein crystallization: Techniques, strategies and tips.* International University Line, La Jolla, USA.

Berman, H. M., Westbrook, J., Feng, Z., Gilliland, G., Bhat, T. N., Weissig, H., Shindyalov, I. N. & Bourne, P. E. (2000). *Nucleic Acids Res*. **28**, 235–242.

Bidmanova, S., Chaloupkova, R., Damborsky, J., Prokop, Z. (2010). *Anal. Bioanal. Chem.* In press. DOI: 10.1007/s00216-010-4083-z.

Bosma, T., Damborsky, J., Stucki, G. & Janssen, D. B. (2002). *Appl. Env. Microbiol.* **68**, 3582-3587.

Bosma, T., Pikkemaat, M., G., Kingma, J., Dijk, J. & Janssen, D., B. (2003). *Biochemistry* **42**, 8047–8053.

Brünger, A. T. (1992). *Nature* **355**, 472–474.

Campbell, D. W., Muller, C. & Reardon, K. F. (2006). *Biotechnol. Lett.* **28**, 883–887.

Chovancova, E., Kosinski, J., Bujnicki, J. M. & Damborsky, J. (2007). *Proteins* **67**, 305–316.

Clegg, W. (1998). *Crystal structure determination*. Oxford University Press, Oxford, 84 pp.

Damborsky, J., Koca, J. (1999). *Protein Eng. Des. Sel.* **12***,* 989–998.

Janssen, D. B. (2004). *Cur. Opin. Chem. Biol.* **8**, 150–159.

Janssen, D. B., Schanstra, J. P. (1994). *Cur. Opin. Biotechnol.* **5**, 253–259.

Janssen, D. B., Dinkla, I. J. T., Poelarends, G. J. & Terpstra, P. (2005). *Environ. Microbiol* **7***,* 1868–1882.

Janssen, D. B., Pries, F. & Van der Ploeg, J. R. (1994). *Annu. Rev. Microbiol*. **48**, 163–191.

Jesenska, A., Sykora, J., Olzynska, A., Brezovsky, J., Zdrahal., Z., Damborsky, J. & Hof, M. (2009). *J. Am. Chem. Soc.* **131** (2), 494–501.

Klvana, M., Pavlova, M., Koudelakova, T., Chaloupkova, R., Dvorak, P., Prokop, Z., Stsiapanava, A., Kuty, M., Kuta-Smatanova, I., Dohnalek, J., Kulhanek, P., Wade, R.C., Damborsky, J. (2009). *J. Mol. Biol.* **392**, 1339–1356.

Kulakova, A. N., Larkin, M. J. & Kulakov, L. A. (1997). *Microbiology* **143**, 109–115.

Long, F., Vagin, A. A., Young, P., Murshudov, G. N. (2007). *Acta Cryst*. D**64**, 125–132.

McPherson, A. (1999). *Crystallization of biological macromolecules*. Cold Spring Harbor Laboratory Press, New York, 586 pp.

McPherson, A. (2002). *Introduction to macromolecular crystallography*, John Wiley & Sons, Inc., 248 pp.

Nardini, M., Dijsktra, B. W. (1999). *Curr. Opin. Struct. Biol.* **9**, 732–737.

Newman, J., Peat, T. S., Richard, R., Kan, L., Swanson, P. E., Affholter, J.A., Holmes, I. H., Schindler, J. F., Unkefer C. J. & Terwilliger, T. C. (1999). *Biochemistry* **38,** 16105–16114.

Ollis, D. L., Cheah, E., Cygler, M., Dijkstra, B., Frolow, F., Franken, S. M., Harel, M., Remington, S. J., Silman, I., Schrag, J., Sussman, J. L., Verschueren, K. H. G., Goldman, A. (1992). *Protein Eng.* **5**, 197–211.

Otyepka M., Damborsky J. (2002). *Protein Sci.* **11**, 1206–1217.

Pavlova, M., Klvana, M., Prokop, Z., Chaloupkova, R., Banas, P., Otyepka, M., Wade, R. C., Tsuda, M., Nagata, Y. & Damborsky J. (2009). *Nature Chem. Biol.* 5, 727–733.

Petrek, M., Otyepka, M., Banas, P., Kosinova, P., Koca, J. & Damborsky, J. (2006) *BMC Bioinformatics* **7**: 316.

Pries, F., Van der Wijngaard, A. J., Bos, R., Pentenga, M. & Janssen, D. B. (1994a). *J. Biol. Chem.* **269**, 17490–17494.

Pries, F., Van der Ploeg, J. R., Dolfing, J. & Janssen, D. B. (1994b). *FEMS Microbiol. Rev.* **15**, 277–295.

Prokop, Z., Damborsky, J., Nagata, Y., & Janssen, D. B. (2004). Patent WO 2006/079295 A2.

Prokop, Z., Damborsky, J., Oplustil, F., Jesenska, A. & Nagata, Y. (2005). Patent WO 2006/128390 A1.

Prokop, Z., Oplustil, F., DeFrank, J. & Damborsky, J. (2006). *Biotech. J.* **1**, 1370–1380.

Prokop Z., Sato Y., Brezovsky J., Mozga T., Chaloupkova R., Koudelakova T., Jerabek P., Stepankova V., Natsume R., Leeuwen J. G. E., Janssen D. B., Florian J., Nagata Y., Senda T., Damborsky J. (2010). *Angew. Chem. Int. Ed.* **49**, 6111–6115.

Rhodes, G. (2006). *Crystallography made crystal clear*. – 3rd ed., Academic Press., 352 pp.

Stsiapanava, A., Dohnalek, J., Gavira, J., A., Kuty, M., Koudelakova, T., Damborsky, J., Smatanova, I., K. (2010). *Acta Cryst*. D**66**, 962–969.

Stucki, G. & Thuer, M. (1995). *Environ. Sci. Technol.* **29**, 2339–2345.

Swanson, P. E. (1999). *Cur. Opin. Biotechnol.* **10**, 365–369.

Swanson, P. E. (1994). Patent US 5 372 944.

Verschueren, K. H. G., Seljee, F., Rozeboom, H. J., Kalk, K. H. & Dijkstra, W. (1993). *Nature* **363**, 693–698.

Wilmanns, M. & Weiss, M. S. (2005*). Molecular Crystallography. Encyclopedia of Condensed Matter Physics*, Academic Press, pp. 453–458.

http://www.pdb.org

Paper I

Crystals of DhaA mutants from *Rhodococcus rhodochrous* NCIMB 13064 diffracted to ultrahigh resolution: crystallization and preliminary diffraction analysis

Reproduced with permission from

Stsiapanava, A., Koudelakova, T., Lapkouski, M., Pavlova, M., Damborsky, J. and Kuta Smatanova, I., *Acta Crys.,* F**64**, 137-140 (2008)

Paper II

Pathways and Mechanisms for Product Release in the Engineered Haloalkane Dehalogenases Explored using Classical and Random Acceleration Molecular Dynamics Simulations

Reproduced with permission from

Klvana, M., Pavlova, M., Koudelakova, T., Chaloupkova, R., Dvorak, P., Stsiapanava, A., Kuty, M., Kuta Smatanova, I., Dohnalek, J., Kulhanek, P., Wade, R. C. and Damborsky, J., *J. Mol. Biol.* **392**, 1339-1356 (2009)

Paper III

Atomic resolution studies of engineered haloalkane dehalogenases DhaA04, DhaA14 and DhaA15 carrying mutations in access tunnels

Reproduced with permission from

Stsiapanava, A., Dohnalek, J., Gavira, J. A., Kuty, M., Koudelakova, T., Damborsky, J. and Kuta Smatanova, I., *Acta Cryst*. D**66,** 962-969 (2010)

Paper IV

Crystallization and preliminary X-ray diffraction analysis of the wild type haloalkane dehalogenase DhaA and the variant DhaA13 complexed with different ligands

Stsiapanava, A., Chaloupkova, R., Jesenska, A., Brynda, J., Weiss, M. S., Damborsky, J. and Kuta Smatanova, I., *manuscript submitted to Acta CrystF* (2010)

Paper V

Crystallization and crystallographic analysis of the *Rhodococcus rhodochrous* NCIMB 13064 mutant DhaA31 and its complex with 1, 2, 3-trichloropropane

Lahoda, M., Chaloupkova, R., Stsiapanava, A., Damborsky, J. and Kuta Smatanova, I., *manuscript prepared for submission* (2010)